Science Signaling
AAAS

www.sciencesignaling.org/cgi/content/full/5/208/ra8/DC1

Supplementary Materials for

Extracellular Ca^{2+} Acts as a Mediator of Communication from Neurons to Glia

Arnulfo Torres, Fushun Wang, Qiwu Xu, Takumi Fujita, Radoslaw Dobrowolski, Klaus Willecke, Takahiro Takano, Maiken Nedergaard*

*To whom correspondence should be addressed. E-mail: nedergaard@urmc.rochester.edu

Published 24 January 2012, *Sci. Signal.* **5**, ra8 (2012)
DOI: 10.1126/scisignal.2002160

The PDF file includes:

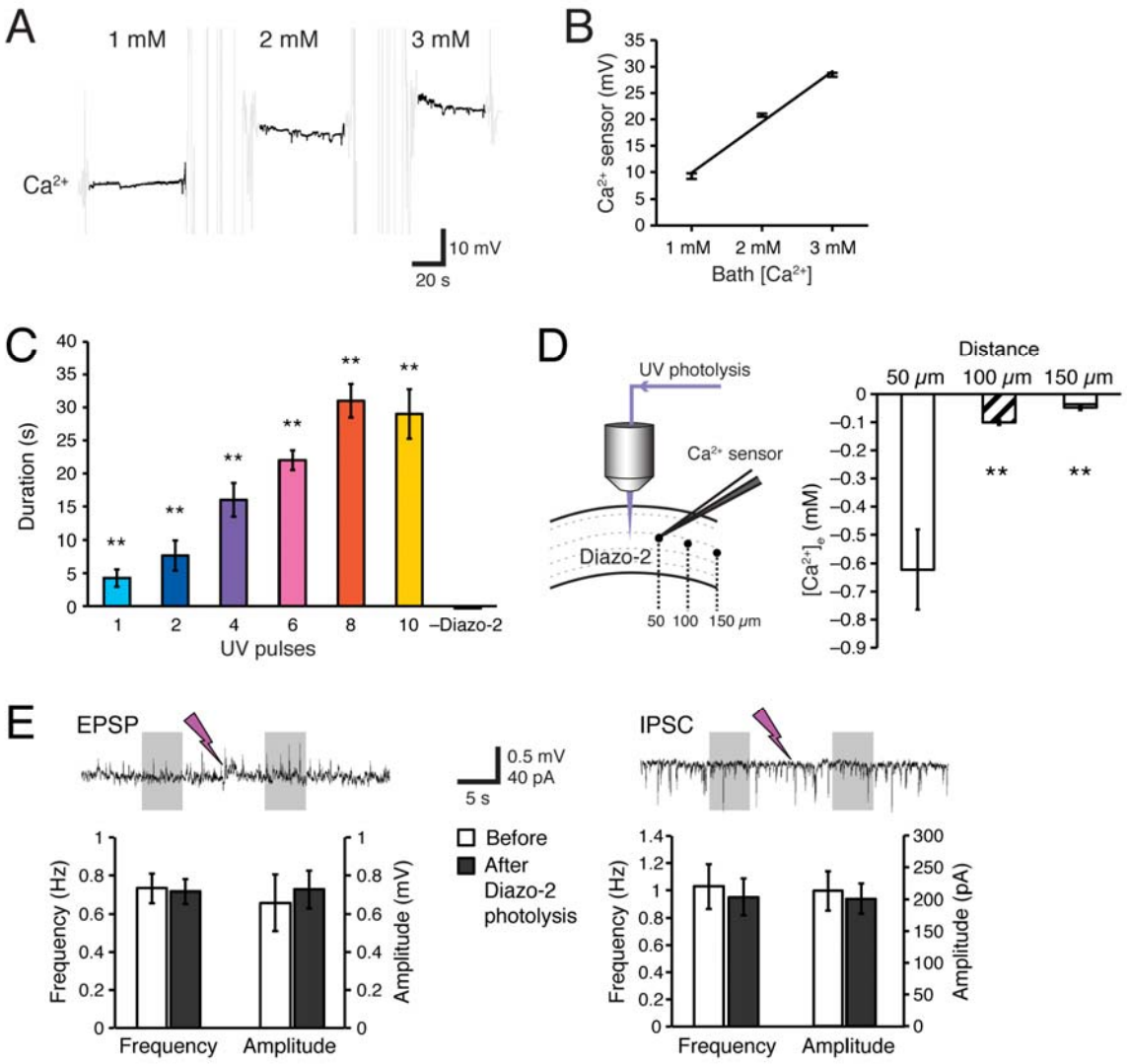

Fig. S1. Calibration of Ca^{2+}-sensitive microelectrode and effects of diazo-2 photolysis on $[Ca^{2+}]_e$

(**A**) Representative trace of calibration of a Ca^{2+}-sensitive microelectrode. Extracellular Ca^{2+} in the bath was successively increased from 1, to 2, to 3 mM Ca^{2+} in aCSF. (**B**) Calibration of Ca^{2+} sensitive microelectrodes in aCSF (n=3 microelectodes, r^2=0.986). The electrodes used in experiments typically showed voltage responses of 5-10 mV per mM increase in Ca^{2+} concentration in the concentration range studied. Electrode calibration was done before and after each experiment. (**C**) Duration of diazo-2-induced decrease in $[Ca^{2+}]_e$ plotted as a function of stimulus intensity (n=3 photolysis events, UV pulses 1-10, and 10 pulses without diazo-2, **, p<0.01). (**D**) Diagram showing recordings obtained by placing the electrode at increasing distances from the photolysis site. Diazo-

2-induced reduction in $[Ca^{2+}]_e$ detected with the Ca^{2+}-sensitive microelectrode placed 50, 100, or 150 µm from the site targeted by photolysis. (n=8 photolysis events, **, $p<0.01$ compared to 50 µm). (**E**) Traces show representative recordings of spontaneous EPSPs and IPSCs in hippocampal CA1 neurons. Bar histograms compare the frequency and amplitude of EPSPs and IPSCs 5 s before or 5 s after photolysis (no significant differences in EPSP or IPSC frequency and amplitude was identified using paired t-test, before vs. after, $p>0.05$, $n = 7$).

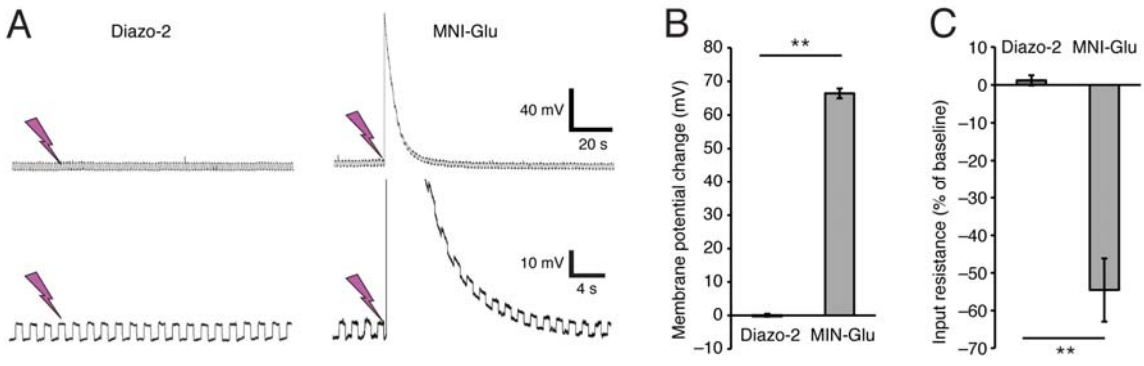

Fig. S2. CA1 pyramidal neurons depolarize and decrease their input resistance in response to photolysis of MNI-glutamate, whereas photolysis of diazo-2 is not associated with changes in the membrane properties

(**A**) Representative current-clamp recordings from a hippocampal CA1 pyramidal cell located ~70 µm from the site of photolysis of diazo-2 (left panel) or MNI-glutamate (right panel). Lower traces show expanded timescale. (**B**) Comparison of changes in plasma membrane potential in response to photolysis of diazo-2 and MNI-glutamate in CA1 pyramidal neurons (n=4-11 photolysis events, **, $p<0.001$). (**C**) Comparison of relative changes in input resistance in response to photolysis of diazo-2 and MNI-glutamate in CA1 pyramidal neurons (n=4-5 photolysis events, **, $p<0.001$).

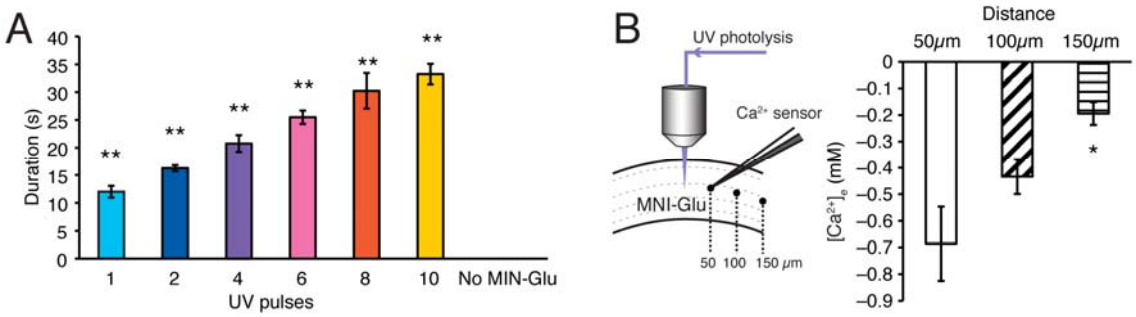

Fig. S3. Photolysis of MNI-glutamate

(A) Duration of the decrease in $[Ca^{2+}]_e$ produced by photolysis of MNI-glutamate plotted as a function of number of UV pulses used for photolysis (n=5 photolysis events, **, $p<0.01$). (**B**) Diagram of recordings obtained by placing the electrode at increasing distances from the photolysis site. MNI-glutamate-induced reduction in $[Ca^{2+}]_e$ detected with the Ca^{2+}-sensitive microelectrode placed 50, 100, or 150 µm from the site targeted by photolysis (n=4-15 photolysis events. *, $p<0.05$ compared to 50 µm). If MNI-glutamate was omitted, UV pulses failed to decrease $[Ca^{2+}]_e$.

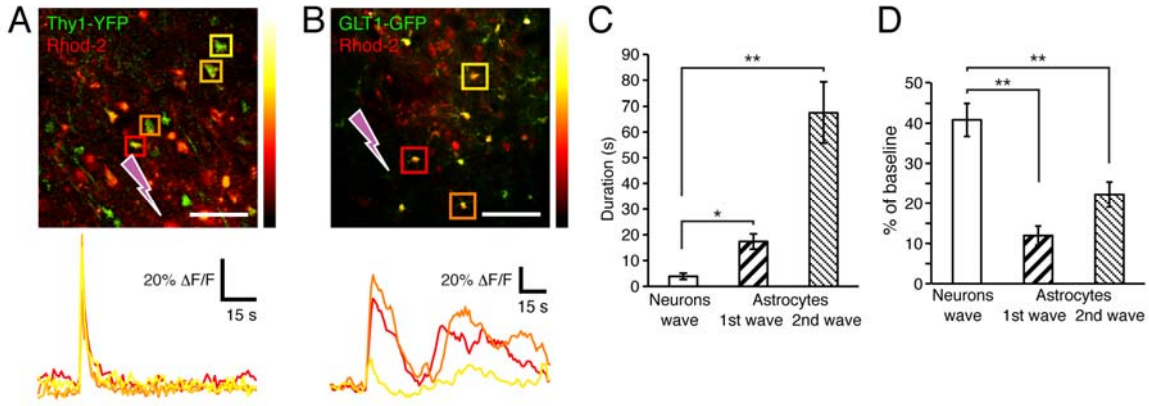

Fig. S4. Transgenic reporter mice reveal distinct responses to MNI-glutamate photolysis of neurons and astrocytes in hippocampal slices

(**A**) Hippocampal slice from a Thy1-YFP reporter mouse loaded with the Ca^{2+} indicator rhod-2 am. YFP+ neurons show an increase in Ca^{2+} during the 1st, but not the 2nd Ca^{2+} wave. Scale bar, 50 µm. (**B**) Hippocampal slice from a GLT1-GFP reporter mouse loaded with the Ca^{2+} indicator rhod-2 am. GFP+ astrocytes show an increase in Ca^{2+} during both the 1st and the 2nd Ca^{2+} waves. Scale bar, 50 µm. (**C**) Duration of the increase in Ca^{2+} in astrocytes and neurons during the 1st and the 2nd Ca^{2+} wave (n=12-13 photolysis events, *, $p<0.05$, **, $p<0.01$). (**D**) The amplitude of the increases in Ca^{2+} in astrocytes or neurons during the 1st or the 2nd Ca^{2+} wave (n=10 photolysis events, **, $p<0.01$).

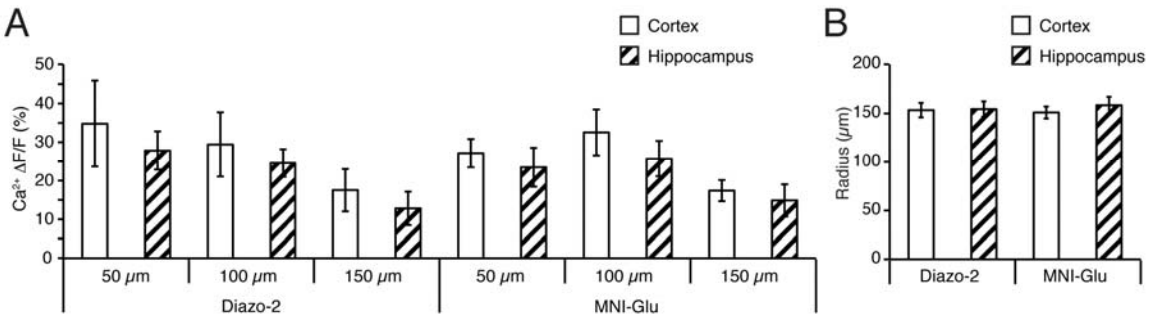

Fig. S5. Comparison of Ca^{2+} waves in hippocampus and cortex evoked by photolysis of MNI-glutamate or diazo-2

(**A**) Comparison of Ca^{2+} increases in astrocytes during the 2nd Ca^{2+} wave evoked by photolysis of MNI-glutamate and the Ca^{2+} wave evoked by photolysis of diazo-2 at 50, 100, and 150 µm in cortex and hippocampus (n=9 photolysis events, $p>0.05$). (**B**) Comparison of maximal radius of the Ca^{2} waves in astrocytes evoked by photolysis of MNI-glutamate and diazo-2 in cortex and hippocampus (n=10 photolysis events, $p>0.05$).

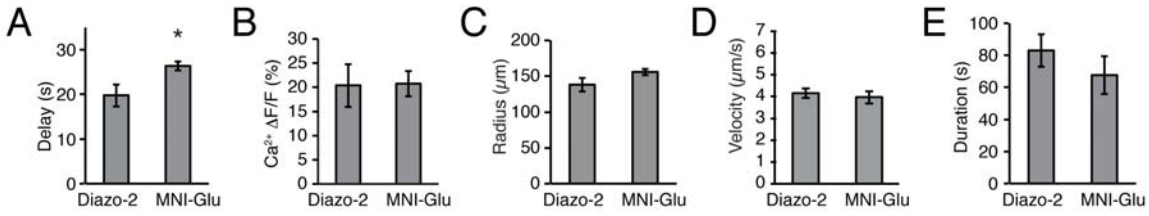

Fig. S6. Comparison of Ca^{2+} waves evoked by diazo-2 or MNI-glutamate photolysis

All comparisons are made between Ca^{2+} waves evoked by diazo-2 photolysis and the 2nd Ca^{2+} wave evoked by MNI-glutamate. (**A**) Histogram comparing the delay between photolysis and the first increase in Ca^{2+} evoked by diazo-2 or MNI-glutamate photolysis (n=20-22 photolysis events, *, $p<0.05$). (**B**) Ca^{2+} increase at 75 µm evoked by diazo-2 or MNI-glutamate photolysis (n=16 photolysis events). (**C**) Radius of Ca^{2+} waves evoked by diazo-2 or MNI-glutamate photolysis (n=26 photolysis events). (**D**) Velocity of Ca^{2+} waves evoked by diazo-2 or MNI-glutamate photolysis (n=18 photolysis events). (**E**) Duration of Ca^{2+} increases in astrocytes evoked by diazo-2 or MNI-glutamate photolysis (n=12 photolysis events).

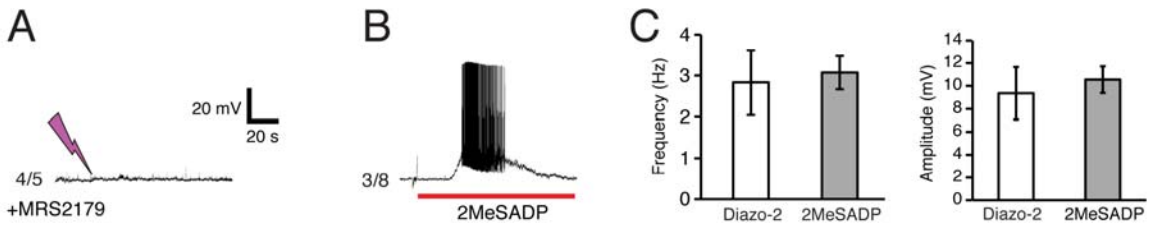

Fig. S7. Effect of manipulation of P2Y1 receptors in hippocampal interneurons

(**A**) The P2Y1 receptor antagonist, MRS2179 (50 µM) blocked depolarization and bursting activity induced by diazo-2 photolysis in 4 of 5 interneurons. One of the five interneurons exhibited a transient minor depolarization, but no action potential firing. (**B**) Exposure to the P2Y1 receptor agonist 2MeSADP (100 µM) induced depolarization in a total of 8 interneurons tested, whereof 3 exhibited bursting activity. (**C**) Histograms compare the frequency of interneuronal action potential firing, as well as the amplitude of membrane depolarization induced by photolysis of diazo-2 with or without exposure to 2MeSADP (n = 6-8 photolysis events).